

# Photopolymerization and Mass-Independent Sulfur Isotope Fractionations in Carbon Disulfide

Jonah J. Colman, Xianping Xu, Mark H. Thiemens,\*  
William C. Trogler\*

Irradiation of gaseous carbon disulfide [ $\text{CS}_{2(g)}$ ] at 313 nanometers produces a dark brown aerosol of  $(\text{CS}_2)_x$ . Its thermal decomposition products include disulfur ( $\text{S}_2$ ), carbon monosulfide ( $\text{CS}$ ), and  $(\text{CS})_x$ . The photopolymerization process is accompanied by a large mass-independent isotopic fractionation of sulfur (a 5 to 10 per mil sulfur-33 excess and a 61 to 84 per mil sulfur-36 deficit). Excess sulfur-33 has been observed in several classes of meteorites. Photochemical production of  $(\text{CS}_2)_x$  may be important in the origin and evolution of cosmochemical environments such as the presolar nebula, meteorites, asteroids, and planetary atmospheres.

Carbon disulfide ( $\text{CS}_2$ ) is a molecule that, on the basis of its thermochemical properties and redox state, could be present in several cosmochemical environments. In July 1994, fragments of comet Shoemaker-Levy 9 (SL9) collided with Jupiter. Observations of this event provided a test for theoretical models of the chemistry of the jovian atmosphere. There were many unexpected results, including the observation of  $\text{CS}_2$ , large amounts of disulfur ( $\text{S}_2$ ) and carbon monosulfide ( $\text{CS}$ ), and the presence of dark aerosol particles in the jovian atmosphere (1, 2). Several comets contain  $\text{CS}_2$  (3) and it could contribute to their chemical reaction network. It appears that  $\text{CS}_2$  condenses as a pristine cometary component and is released as a comet nears the sun. This observation suggests that substantial amounts of  $\text{CS}_2$  exist in comet-forming regions. Meteoritic S isotopic measurements document the presence of excess  $^{33}\text{S}$  in S-bearing organic molecules (4), bulk ureilites (5), and acid residues of Allende carbonaceous chondrites (6). The latter measurements are intriguing, because they suggest a relation between noble gas isotopic anomalies in ureilites and carbonaceous chondrite acid-resistant residues (7). Because these acid residues (phase Q) may be carriers of planetary noble gases, there is interest in the chemical origins of these S-bearing carbonaceous phases.

Carbon disulfide polymerizes into a black solid  $(\text{CS}_2)_x$  at 40 kbar and 425 K (8). Recently, it was determined that aerosols of  $(\text{CS}_2)_x$  are also produced by long-wavelength (280 to 370 nm) ultraviolet (UV) irradiation of  $\text{CS}_{2(g)}$  (9). Because  $\text{CS}_2$  is an important S-bearing molecule under nebular or cometary conditions (10) and because

the volatile thermal fragmentation products of  $(\text{CS}_2)_x$  resemble those observed during the collision of SL9 with the jovian atmosphere, we undertook chemical and isotopic studies. The addition of an atmosphere of molecular nitrogen ( $\text{N}_2$ ) or molecular hydrogen ( $\text{H}_2$ ) to  $\text{CS}_2$  does not affect the photopolymerization reaction. The quantum yield for photopolymerization is first-order in  $\text{CS}_2$ ; at 0.2 torr (buffered to 1 atm with  $\text{N}_2$  or  $\text{H}_2$ ) it is approximately  $10^{-2}$ . The measurement was complicated by the formation of scattering aerosols and absorbing films [for example, the  $(\text{CS}_2)_x$  film shown in Fig. 1] that reduce the radiation received by the  $\text{CS}_{2(g)}$ . Particle production was observed at mixing ratios as low as 300 parts per million (ppm), film growth at mixing ratios as low as 145 ppm, and photooxidation at mixing ratios as low as 10 ppm.

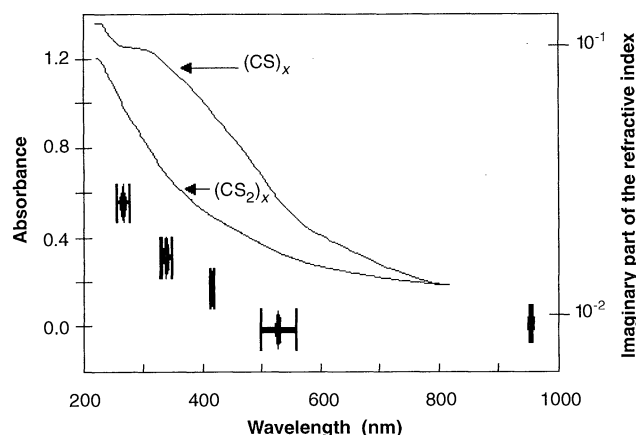
Irradiation of  $(\text{CS}_2)_x$  with an unfiltered, high-pressure, 250-W Hg-Xe arc lamp (wavelength  $\lambda > 230$  nm) in vacuum or under an atmosphere of  $\text{N}_2$  or  $\text{H}_2$  did not generate any new infrared (IR) active gas-phase species or change the IR spectrum of the  $(\text{CS}_2)_x$ . This behavior contrasts with

the behavior of  $(\text{CS}_2)_x$  in an oxidizing ( $\text{O}_2$ ) atmosphere where  $(\text{CS}_2)_x$  undergoes photooxidation ( $\lambda < 480$  nm) to produce carbon monoxide ( $\text{CO}$ ), carbonyl sulfide ( $\text{OCS}$ ), sulfur dioxide ( $\text{SO}_2$ ), elemental S, and a polymer that has incorporated O (9). The  $(\text{CS}_2)_x$  polymer is stable in strong acids and bases, and it is insoluble in common laboratory solvents.

We investigated the thermal stability of  $(\text{CS}_2)_x$  by direct port-injection mass spectrometry. Decomposition begins at 428 K, and it is relatively fast at 473 K. The predominant mass peaks observed in these experiments were attributable to disulfur ( $\text{S}_2$ ) and lesser amounts of CS. Trace amounts of  $\text{CS}_2$  and higher molecular weight S species ( $\text{S}_3$  through  $\text{S}_8$ ) were also observed. The extruded  $\text{S}_2$  fragment agrees with the structure postulated for  $(\text{CS}_2)_x$ , which is based on chains of CS cross-linked with disulfide bridges (9). A black residue typically remains after thermolysis. Heating  $(\text{CS}_2)_x$  in a sublimator (543 to 563 K) for 4 hours under vacuum yields a black residue with the approximate composition of  $(\text{CS})_x$  (11).

Carbon disulfide exhibits a short-wavelength absorption (185 to 215 nm) that causes photodissociation and a long-wavelength (280 to 370 nm) feature. The ratio of short-wavelength excitation (185 to 215 nm) to long-wavelength excitation (280 to 370 nm) of  $\text{CS}_2$  is about 100. This estimate is based on recent  $\text{CS}_2$  extinction coefficient measurements (12, 13), treats the sun as a blackbody at 5780 K, and assumes that there are no other absorbing species. However, in a planetary atmosphere, the optical opacity is typically much greater in the shorter wavelength region than at 280 to 370 nm. Thus, there will be a greater proportion of 313-nm electronic excitation in an atmospheric environment than in free space. For example, the photodissociative lifetime estimated for  $\text{CS}_2$  at 5.2 astronomical units (the distance between Jupiter and the sun) is 4.4 hours (3). In the jovian

**Fig. 1.** Ultraviolet-visible spectra of thin films of  $(\text{CS}_2)_x$  and  $(\text{CS})_x$  (values given on the left) and the imaginary part of the refractive index of the particles observed in the jovian atmosphere (values given in logarithmic scale on the right) as modeled by West *et al.* (2). The horizontal location and size of the symbols indicate the filter wavelengths and the size of the passband. The vertical size of the symbols indicates the range of values that were able to fit the observations.



Department of Chemistry and Biochemistry, University of California at San Diego, La Jolla, CA 92093-0358, USA.

\*To whom correspondence should be addressed.

atmosphere, the lifetime would be 8.2 hours at  $10^{-5}$  mbar (14) and  $\approx 1$  week at 1 mbar (15). In the terrestrial atmosphere, photodissociation of  $\text{CS}_2$  is negligible below 5 to 6 km (16). Thus, the lifetime of  $\text{CS}_2$  before dissociation is long enough in many planetary atmospheres to allow photopolymerization to occur.

The collision of comet SL9 with Jupiter provided indirect evidence that  $(\text{CS}_2)_x$  may be present either in the jovian atmosphere or in the comet itself. Large amounts of  $(\text{CS}_2)_x$  thermal fragmentation products ( $\text{S}_2$ ,  $\text{CS}$ , and  $\text{CS}_2$ ) were observed near the impact sites. These were not predicted by current models of the jovian atmosphere. Early reports suggested that the quantity of S species observed implies a jovian origin for the  $\text{S}_2$ , but this result is still uncertain. Carbon monosulfide was not observed outgassing from comet SL9 before the collision (17). However, CS has been observed in the atmospheres of other comets (18), and it is thought to arise from  $\text{CS}_2$  photodissociation at 185 to 215 nm (3, 19). Free  $\text{CS}_2$  was not observed in the jovian atmosphere by the recent Galileo probe (20).

We produced a  $(\text{CS}_2)_x$  film by irradiating  $\text{CS}_2$  vapor at 20 torr and allowing it to deposit on the quartz cell window. The  $(\text{CS}_2)_x$  film was produced by thermolysis of a  $(\text{CS}_2)_x$  film (4 hours at 550 K, under vacuum). The spectra show that both  $(\text{CS}_2)_x$  and  $(\text{CS})_x$  absorb strongly over the entire visible spectrum (Fig. 1). Reflectance measurements show that  $(\text{CS}_2)_x$  reflects relatively more than  $(\text{CS})_x$  above 600 nm. This result is consistent with the observed dark red-brown color of  $(\text{CS}_2)_x$  and the black appearance of  $(\text{CS})_x$ . Reflectance spectra of the jovian atmosphere share some of these characteristics.

The observed dark brown impact debris particles from SL9 have been investigated for their reflectivity (2). The calculated imaginary refractive index is about 0.008 between 1000 and 550 nm, then slopes upward to about 0.02 at 250 nm (Fig. 1). The imaginary refractive indices (directly proportional to the extinction coefficients) of  $\text{H}_2\text{O}$ , ammonia ( $\text{NH}_3$ ), and carbon dioxide ( $\text{CO}_2$ ) are too small to account for such absorption over the entire spectral range of observations. Molecular S is not sufficiently absorbing over the spectral range to account for the results. The shapes of ratio spectra taken of the SL9 impact region at different times require the presence of a postimpact continuum absorber (1). The data could be explained if some of the aerosol in the jovian atmosphere were  $(\text{CS}_2)_x$  and it underwent thermal decomposition to polymeric  $(\text{CS})_x$  residue, free CS, and  $\text{S}_2$  near the site of impact. The  $(\text{CS}_2)_x$  aerosol could have formed initially in the reducing jovian atmo-

sphere through long-wavelength ultraviolet (UV) photopolymerization of  $\text{CS}_2$ .

An isotopic study of  $(\text{CS}_2)_x$  provides further evidence that this species may be important in cosmochemical environments. There is an enormous heavy-isotope enrichment, ranging from  $\delta^{34}\text{S} = 45$  per mil for UV lamp irradiation to  $\delta^{34}\text{S} = 56.5$  per mil for solar photolysis (21, 22). More important, the isotopic fractionation pattern is mass-independent. For S, a conventional mass-dependent isotopic fractionation process yields  $\delta^{33}\text{S} = 0.5 \delta^{34}\text{S}$  and  $\delta^{36}\text{S} = 0.51 \delta^{34}\text{S}$  (22) (Fig. 2, A and B). By convention, deviations from the mass-dependent fractionation are reported as  $^{33}\Delta = \delta^{33}\text{S} - 0.5 \delta^{34}\text{S}$  and  $^{36}\Delta = \delta^{36}\text{S} - 1.97 \delta^{34}\text{S}$  (22). The  $^{33}\text{S}$  excess ranges from a  $^{33}\Delta$  of 5.3 per mil in the laboratory photolysis experiments to 10.8 per mil for the solar experiments. For  $^{36}\text{S}$ ,  $^{36}\Delta = -61$  per mil and  $-82.5$  per mil for the laboratory photolysis and solar irradiation, respectively.

The experiments show that anomalous  $^{33}\text{S}$  enrichments and  $^{36}\text{S}$  deficiencies can be produced by long-wavelength UV photolysis of  $\text{CS}_2$ . This may be an important process in a nebular environment because (i)  $\text{CS}_2$  is a dominant S-bearing molecule in nebulae (10), (ii) photopolymerization by solar irradiation produces the greatest isotopic fractionation, and (iii) the isotopic anomaly is similar to that found in meteorites (4–6). The actinic radiation occurs in a spectral region where few other simple gaseous molecules absorb and could be provided by early solar irradiation or background stellar photolysis. The magnitude of the observed  $^{33}\text{S}$  excess is small enough that a concomitant  $^{36}\text{S}$  deficiency may have escaped detection (at the decreased isotopic sensitivity for the low-abundance  $^{36}\text{S}$  measurements). In the ureilites, sulfides are commonly found intergrown with euhedral graphite crystals (23). This result suggests a potential chemical association between C and S in ureilites, where  $^{33}\text{S}$  anomalies are found at bulk levels. If the  $(\text{CS}_2)_x$  material were produced under nebular conditions and incorporated into the ureilite parent body, the  $^{33}\text{S}$  enrichment and a C-S relation would result. Secondary planetary differentiation, such as might occur on the ureilite parent body (24), could produce the graphite-metal-sulfide assemblage.

An anomalous black polymeric material, known to be the carrier of noble gases (phase Q) and  $^{33}\text{S}$  excesses in Allende, also resides in ureilites (7). Phase Q has chemical characteristics similar to those of the  $(\text{CS}_2)_x$  material, including its insolubility and chemical resistance to acid treatment. The physical-chemical characteristics of Q and  $(\text{CS}_2)_x$ , and the presence of Q in the two meteorite classes containing  $^{33}\text{S}$  excesses, suggest that

the process reported here could be responsible in part for the generation of Q.

An environment that includes  $\text{CS}_2$  and 313-nm radiation will eventually produce  $(\text{CS}_2)_x$ . A limitation in the chemistry is the lifetime of the initiating electronic state. The lifetimes (25, 26) of the known fluorescent states of  $\text{CS}_2$  are insufficient to allow them to cause photopolymerization at mixing ratios below 1%; however,  $(\text{CS}_2)_x$  aerosols are seen at mixing ratios as low as 300 ppm. Formation of OCS in mixtures of  $\text{CS}_2$  and molecular oxygen ( $\text{O}_2$ ) occurs largely by secondary photolysis of  $(\text{CS}_2)_x$ , and this is observed at mixing ratios as low as 10 ppm. Photopolymerization must therefore arise from a longer lived electronic state. There is tentative evidence that the fluorescent states are strongly coupled to nearby nonradiative states (27, 28).

There is no known physical-chemical mechanism that readily accounts for the simultaneous enrichment and depletion of S isotopes observed in  $(\text{CS}_2)_x$ . The results are inconsistent with a symmetry-dependent isotope effect, as has been observed in several other reactions (23). A symmetry dependence would predict equal enrichments in  $^{33}\text{S}$ ,  $^{34}\text{S}$ , and  $^{36}\text{S}$ . The observed  $\delta^{33}\text{S}/\delta^{34}\text{S}$  ratios range from 0.62 to 0.7 rather than having a value of 1.0, and the  $^{36}\text{S}$  nuclide is depleted. Nuclear spin effects do not appear to be involved, because only  $^{33}\text{S}$  has a spin moment. The mechanism may involve differing rates of nonradiative transfer from the

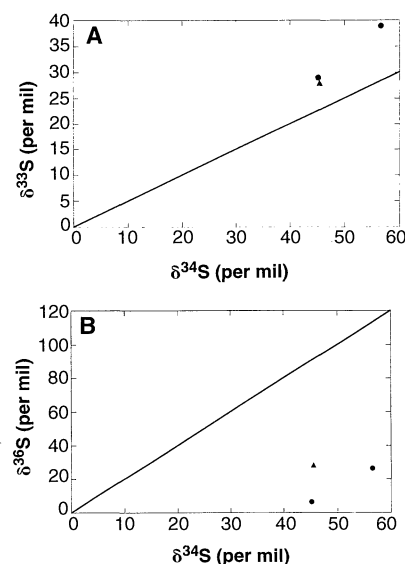


**Fig. 2.** Three-isotope plots for the  $(\text{CS}_2)_x$  produced by near-UV ( $\blacktriangle$ ) and solar radiation photolysis ( $\bullet$ ). The mass fractionation lines are included in each plot. Data are normalized to a starting  $\text{CS}_2$  isotopic composition of  $\delta^{33}\text{S} = \delta^{34}\text{S} = \delta^{36}\text{S} = 0$ . (A)  $\delta^{33}\text{S}$  versus  $\delta^{34}\text{S}$ . (B)  $\delta^{36}\text{S}$  versus  $\delta^{34}\text{S}$ . The slope of the line in (A) is 1/2. The slope of the line in (B) is 2.

initial absorbing state to the reactive state. Such rates could depend on the Franck-Condon factors between specific rotational-vibrational levels in the two states.

## REFERENCES AND NOTES

1. K. S. Noll *et al.*, *Science* **267**, 1307 (1995).
2. R. A. West *et al.*, *ibid.*, p. 1296.
3. W. M. Jackson, P. S. Butterworth, D. Ballard, *Astrophys. J.* **304**, 515 (1986).
4. G. W. Cooper *et al.*, *Meteoritics* **30**, 500 (1995).
5. M. H. Thiemens and T. Jackson, *Lunar Planet. Sci. Conf.* **XXVI**, 1405 (1995).
6. C. E. Rees and H. G. Thode, *Geochim. Cosmochim. Acta* **41**, 1697 (1977).
7. R. Wieler *et al.*, *ibid.* **55**, 1709 (1991).
8. P. W. Bridgman, *Proc. Am. Acad. Arts Sci.* **74**, 399 (1941).
9. J. J. Colman and W. C. Trogler, *J. Am. Chem. Soc.* **117**, 11270 (1995).
10. K. Zahnle, M.-M. M. Low, K. Lodders, B. Fegley Jr., *Geophys. Res. Lett.* **22**, 1593 (1995).
11. Elemental analyses were performed by Desert Analytics: 26.72 weight % C and 72.70 weight % S ( $\text{CS}_{1.02}$ ).
12. J. J. Colman and W. C. Trogler, preprint of paper presented at the 207th national meeting of the American Chemical Society, San Diego, CA, March 1994; ENV 67.
13. F. Z. Chen and C. Y. R. Wu, *Geophys. Res. Lett.* **22**, 2131 (1995).
14. J. I. Moses, M. Allen, G. R. Gladstone, *ibid.*, p. 1597.
15. E. Lellouch *et al.*, *Nature* **373**, 592 (1995).
16. M. Chin and D. D. Davis, *Global Biogeochem. Cycles* **7**, 321 (1993).
17. H. A. Weaver *et al.*, *Science* **267**, 1282 (1995).
18. J. Crovisier, D. Despois, D. Bockelée-Morvan, P. Colom, G. Paubert, *Icarus* **93**, 246 (1991).
19. This calculation assumes that the quantum yield for photodissociation equals 1, but this datum does not exist in the literature. Therefore, a direct measurement was undertaken. The quantum yield that we obtained for  $\text{CS}_2$  removal at 193 nm, using an ArF excimer laser and  $\text{N}_2\text{O}$  photodissociation (quantum yield, 1.44; extinction coefficient,  $8.95 \times 10^{-20} \text{ cm}^2$ ) as an actinometer, was 0.5 to 1.
20. H. B. Niemann *et al.*, *Science* **272**, 846 (1996). A small signal was observed at 76 atomic mass units (amu), but no signal was observed at 78 amu. If solar abundances were obtained, there should have been an 8.02% abundance of the 78-amu isotopomer.
21. All  $(\text{CS}_2)_x$  samples used for isotopic analysis were produced in a 2400-ml quartz Schlenk flask. About 1 to 2 ml of  $\text{CS}_2$  was placed in the flask, which then was multiply (three times) freeze-pump-thaw degassed. Photochemical conversions were less than 5% for the isotopic measurements. Sample 1 was irradiated for 100 hours with a Pyrex-filtered 450-W, medium-pressure Hg lamp. The  $(\text{CS}_2)_x$  was collected by suspension in acetone and centrifugation. Sample 2 was prepared by 2 weeks of solar irradiation (late July, 32°N latitude). We dislodged the  $(\text{CS}_2)_x$  from the sides of the flask and collected it on weighing paper. Sample 3 was produced by 8 days of solar irradiation (early October). The polymer was solvent-collected, as for sample 1. The S isotopic composition of the  $(\text{CS}_2)_x$  was determined by procedures described in (22).
22. X. Gao and M. H. Thiemens, *Geochim. Cosmochim. Acta* **57**, 3159 (1993). Isotopic compositions are reported in the conventional delta notation, in which

$$\delta^{34}\text{S} = \left[ \frac{(^{34}\text{S}/^{32}\text{S})_{\text{sample}}}{(^{34}\text{S}/^{32}\text{S})_{\text{standard}}} - 1 \right] \times 1000$$

This quantifies the  $^{34}\text{S}/^{32}\text{S}$  ratio in a sample, referenced to the standard S in CDT (Canyon Diablo triolite). Variations are reported in parts per thousand or per mil. The  $\delta^{33}\text{S}$  ( $^{33}\text{S}/^{32}\text{S}$ ) and  $\delta^{36}\text{S}$  ( $^{36}\text{S}/^{32}\text{S}$ ) ratios were also determined. Errors associated with  $\delta^{33}\text{S}$  and  $\delta^{34}\text{S}$  are  $\pm 0.04$  per mil and  $\pm 0.15$  per mil for  $\delta^{36}\text{S}$ . Figure 2 shows the isotopic results, normalized to the initial  $\text{CS}_2$  isotopic composition ( $\delta^{32}\text{S} = 4.24$ ,

- $\delta^{34}\text{S} = 8.25$ ,  $\delta^{36}\text{S} = 15.26$  with respect to CDT).
23. M. H. Thiemens, in *Isotope Effects in Gas Phase Chemistry*, J. A. Kaye, Ed. (American Chemical Society, Washington, DC, 1992), pp. 138–153.
  24. C. A. Goodrich, *Meteoritics* **27**, 327 (1992).
  25. C. Lambert and G. H. Kimbell, *Can. J. Chem.* **51**, 2601 (1973).
  26. L. E. Brus, *Chem. Phys. Lett.* **12**, 116 (1971).
  27. A. Habib, R. Görger, G. Brasen, R. Lange, W.

Demtröder, *J. Chem. Phys.* **101**, 2752 (1994).

28. A. E. Douglas and E. R. V. Milton, *ibid.* **41**, 357 (1964).
29. We thank A. C. Kummel and E. Lanzendorf for use of the excimer laser. Supported by NSF (grant CHE-931940) and NASA (grants NAGW 3551 and NAGW 2251).

16 April 1996; accepted 10 June 1996

# A Statistical Model of the Fluctuations in the Geomagnetic Field from Paleosecular Variation to Reversal

Pierre Camps\* and Michel Prévot

The statistical characteristics of the local magnetic field of Earth during paleosecular variation, excursions, and reversals are described on the basis of a database that gathers the cleaned mean direction and average remanent intensity of 2741 lava flows that have erupted over the last 20 million years. A model consisting of a normally distributed axial dipole component plus an independent isotropic set of vectors with a Maxwellian distribution that simulates secular variation fits the range of geomagnetic fluctuations, in terms of both direction and intensity. This result suggests that the magnitude of secular variation vectors is independent of the magnitude of Earth's axial dipole moment and that the amplitude of secular variation is unchanged during reversals.

The way the geomagnetic field reverses itself remains poorly understood, because of the scarcity of reliable and sufficiently complete paleomagnetic records of the same reversal from widely distant sites at Earth's surface. Two main questions are still unanswered. First, are field reversals and excursions specific phenomena unrelated to paleosecular variation? Although excursions and reversals are sometimes considered as extrema of secular variation (1), all the statistical field models produced thus far by the paleomagnetic community are restricted to the description of paleosecular variation, which implies that the paleosecular regime (2) is physically distinct from the reversing regime. However, we know of no observation that has confirmed this view.

The second main question regards the composition (ideally, in terms of spherical harmonic coefficients) of the reversing field as compared with that of the so-called "stable" field. Absolute paleointensity data show unambiguously that the field strength is considerably reduced during reversals and excursions (3–6); therefore, a large reduction of the dipole moment is needed. Obviously, the axial dipole (AD) has to pass through zero as the field reverses. Our certainties stop here. The behavior of the equatorial dipole is not known, nor do we

know whether the destiny of the nondipole terms is correlated with that of the dipole. Does the energy of the dipole transfer into that of some other terms (7), or does it reduce without any correlated change in the other terms (8)?

Paleomagnetic data allow an examination of these questions from a statistical standpoint, provided that the paleofield strength is taken into account. For this purpose, we compiled a paleomagnetic database from volcanic rocks that, in contrast to earlier databases (9, 10), includes remanence intensity and covers the entire range of geomagnetic fluctuations, from paleosecular variation to reversal. The use of remanence intensity instead of paleofield strength was forced by the present scarcity of paleointensity data that precludes, in any region of Earth, a proper statistical description of paleofield strength. Assuming that the average remanence intensity is proportional to the average paleofield strength, we propose a statistical model of the local geomagnetic fluctuations. The agreement between our observations and the predictions of this model suggests that the magnitude of secular variation is not connected to the longer term variation of the AD moment.

Geomagnetic field fluctuations are generally analyzed after the local field vector is transformed into a virtual geomagnetic pole (VGP). Here, we use the local geographic reference frame because the VGP transformation becomes less physically significant

Laboratoire de Tectonique et Géophysique, Unité Associée au CNRS case 060, Université de Montpellier 2, Place Eugène Bataillon, 34095 Montpellier Cedex 5, France.

\*To whom correspondence should be addressed.